JBC ARTICLE

Proteolytic cleavage orchestrates cofactor insertion and protein assembly in [NiFe]-hydrogenase biosynthesis

Received for publication, March 24, 2017, and in revised form, May 23, 2017 Published, Papers in Press, May 24, 2017, DOI 10.1074/jbc.M117.788125

Moritz Senger, Sven T. Stripp, and Basem Soboh[1]

From the Department of Physics, Experimental Molecular Biophysics, Freie Universitaet Berlin, 14195 Berlin, Germany

Edited by Ruma Banerjee

Metalloenzymes catalyze complex and essential processes, such as photosynthesis, respiration, and nitrogen fixation. For example, bacteria and archaea use [NiFe]-hydrogenases to catalyze the uptake and release of molecular hydrogen (H_2). [NiFe]-hydrogenases are redox enzymes composed of a large subunit that harbors a $NiFe(CN)_2CO$ metallo-center and a small subunit with three iron–sulfur clusters. The large subunit is synthesized with a C-terminal extension, cleaved off by a specific endopeptidase during maturation. The exact role of the C-terminal extension has remained elusive; however, cleavage takes place exclusively after assembly of the [NiFe]-cofactor and before large and small subunits form the catalytically active heterodimer. To unravel the functional role of the C-terminal extension, we used an enzymatic *in vitro* maturation assay that allows synthesizing functional [NiFe]-hydrogenase-2 of *Escherichia coli* from purified components. The maturation process included formation and insertion of the $NiFe(CN)_2CO$ cofactor into the large subunit, endoproteolytic cleavage of the C-terminal extension, and dimerization with the small subunit. Biochemical and spectroscopic analysis indicated that the C-terminal extension of the large subunit is essential for recognition by the maturation machinery. Only upon completion of cofactor insertion was removal of the C-terminal extension observed. Our results indicate that endoproteolytic cleavage is a central checkpoint in the maturation process. Here, cleavage temporally orchestrates cofactor insertion and protein assembly and ensures that only cofactor-containing protein can continue along the assembly line toward functional [NiFe]-hydrogenase.

More than one-third of all proteins in nature have been shown to bind metal cofactors (1). Metalloenzymes catalyze complex and essential processes, such as photosynthesis, respiration, and nitrogen fixation (2). Industrial interest stems from the excellent catalytic performance and specificity of certain metalloenzymes (*e.g.* in biotechnological and pharmaceutical applications) (3). Furthermore, metalloproteins receive growing attention due to the discovery of numerous diseases related to cofactor biosynthesis (4). Coordination of synthesis and assembly of multisubunit metalloproteins must be tightly controlled to ensure that only correctly folded and catalytically active enzymes are delivered to their subcellular destination. The physiological and molecular orchestration of events (*e.g.* coordination of protein and cofactor synthesis or assembly of cofactors into apoprotein) is not fully understood. Our comprehension of metal cofactor biosynthesis has been facilitated by the study of [NiFe]-hydrogenases, which served as excellent model systems (5, 6). Due to their capability to catalyze the reversible reduction of protons to molecular hydrogen (H_2), hydrogenases have been discussed for potential bioenergy applications and industrial production of H_2 (7).

Typically, [NiFe]-hydrogenases are heterodimers of a large and a small subunit. The "large subunit" binds the catalytic $NiFe(CN)_2CO$ cofactor (8, 9), and the "small subunit" contains three iron–sulfur (FeS) clusters involved in electron transfer. The nickel ion of the bimetallic active site is coordinated via four conserved cysteinyl thiolates, two of which additionally ligate an iron ion. The iron site carries one carbonyl (CO)[2] and two cyanide (CN) ligands. These unique ligands are proposed to maintain the low-spin Fe(II) state important for H_2 activation (10, 11). Fig. 1 presents our current working model for hydrogenase maturation and suggests the following sequence of events: (i) synthesis of CO and CN, ligation to iron, and incorporation of the fully coordinated iron into the large subunit pro-protein by the coordinated activity of HypCDEF (12); (ii) nickel insertion by concerted activity of HypA, HypB, and SlyD (6, 13) (these accessory proteins are not required at high Ni^{2+} concentrations) (5, 14); (iii) nickel acting as recognition site for a specific endopeptidase (15); cleavage of the C-terminal extension of the pro-protein that harbors the [NiFe]-cofactor, inducing conformational changes; and (iv) complex formation with the small subunit to yield active [NiFe]-hydrogenase (16, 17).

Escherichia coli synthesizes three distinct membrane-bound [NiFe]-hydrogenases: hydrogenase-1 (Hya), hydrogenase-2 (Hyb), and hydrogenase-3 (Hyc). The large subunit of each hydrogenases is synthesized as a pro-protein with a C-terminal extension, cleaved off by a specific endopeptidase. Besides the proteins mentioned above (HypABCDEF), orthologous accessory proteins have been described. For example, HybG is involved in delivery of the completed $Fe(CN)_2CO$ moiety to the large subunit of hydrogenase-2, whereas its homologue HypC delivers the cofactor to hydrogenase-3. Table 1 describes the proposed function of [NiFe]-hydrogenase maturation proteins

This work was supported by the Deutsche Forschungsgemeinschaft through the priority program "Iron-Sulfur for Life," Grant SO 1325/5-1 (to B. S.). The authors declare that they have no conflicts of interest with the contents of this article.

[1] To whom correspondence should be addressed: Dept. of Physics, Experimental Molecular Biophysics, Freie Universitaet Berlin, Arnimallee 14, 14195 Berlin, Germany. Tel.: 49-030-838-56098; E-mail: basem.soboh@fu-berlin.de.

[2] The abbreviations used are: CO, carbonyl; CN, cyanide; ICP-MS, inductively coupled plasma mass spectrometry; GDE, HybG–HypDE.

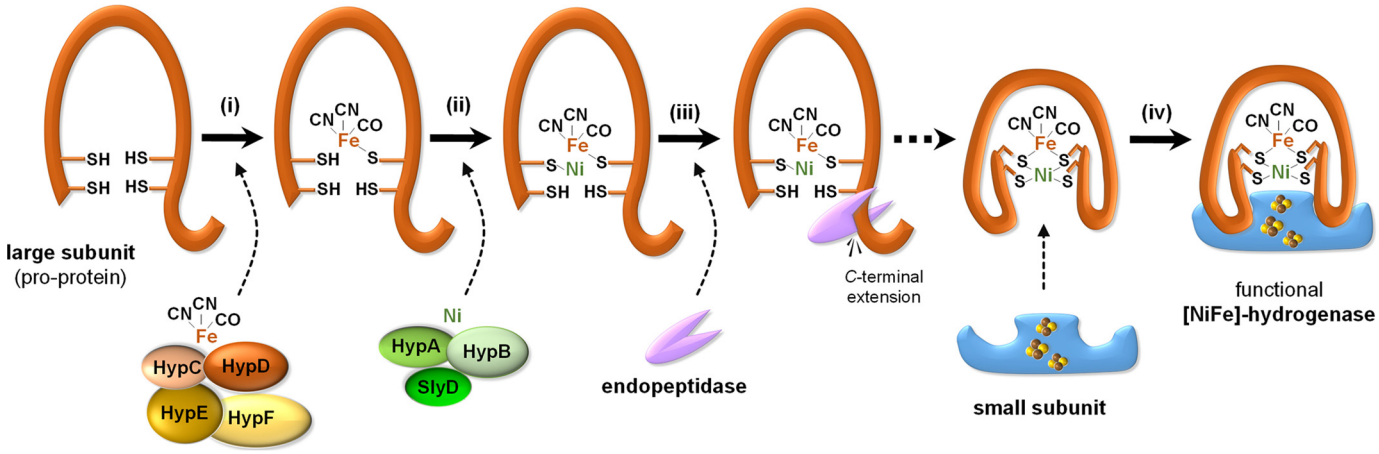

Figure 1. Working model for maturation of the large subunit into functional [NiFe]-hydrogenase. *i*, incorporation of the $Fe(CN)_2CO$ moiety into the hydrogenase large subunit (pro-protein) by the coordinated activity of HypCDEF. *ii*, nickel insertion by concerted activity of HypA, HypB, and SlyD. *iii*, endoproteolytic cleavage of the C-terminal peptide, associated with conformational changes of the protein. *iv*, dimerization of large and small subunit forms functional [NiFe]-hydrogenase.

Table 1
Proteins involved in the maturation process of hydrogenase-2 from *E. coli*

Protein	Molecular mass	Function/Properties
	kDa	
HybC	63.5	Large subunit of hydrogenase-2; contains the [NiFe] active site (50).
HybO	39.6	Small subunit of hydrogenase-2; contains one [3Fe-4S] and two [4Fe-4S] clusters that are involved in electron transfer from or to the active site (52).
HybF (HypA)	12.5	Involved in acquisition and insertion of the nickel into large subunit HybC (53).
HypB	31.5	GTPase activity; binds nickel and forms with SlyD the HypB–SlyD complex that activates nickel release and insertion into the large subunit (54,55).
HybG (HypC)	8.7	Small iron- and CO_2-binding protein; proposed to deliver CO_2 for reduction to CO by HypD (27). Forms with HypD the core complex of hydrogenase-2 maturation machinery (HybG–HypD), that is involved in delivering the completed $Fe(CN)_2CO$ moiety to the large subunit HybC (14).
HypD	41.4	The only FeS cluster-containing Hyp protein; acts as a scaffold for assembly of the $Fe(CN)_2CO$ moiety of the cofactor prior to its transfer to the large subunit (28).
HypE	35	HypE is a homodimer; forms a heterooligomer with HypCD (38) and a heterotetramer with HypF (56). HypEF heterotetramer generates CN ligands from carbamoyl phosphate in an ATP-dependent condensation reaction (25).
HypF	82	Carbamoyl phosphate phosphatase; carbamoyl-transferase; ATPase; involved in CN synthesis (26,57).
HybD	17.6	Endopeptidase; involved in C-terminal cleavage of the hydrogenase-2 large subunit (33).

from *E. coli* used in this study. Most enzymes and substrates involved in biosynthesis and assembly of the bimetallic cofactor have been identified. However, details about the coordination of protein synthesis and cofactor assembly are largely unknown.

To identify the sequence of events in active site biosynthesis and investigate the individual role of each accessory protein, an approach is required that allows reconstructing the maturation pathway. Here, we developed an enzymatic *in vitro* assay to study the synthesis of active [NiFe]-hydrogenase 2 from *E. coli*. The starting point is the unprocessed, large subunit pro-protein (HybC) and five individual [NiFe]-hydrogenase maturation proteins in purified form. The experiments focus on the question of when and why the C-terminal extension of HybC is cleaved off. Making use of biochemical analysis, circular dichroism, and infrared spectroscopy, we found that proteolytic cleavage coordinates cofactor insertion and protein assembly during the maturation of [NiFe]-hydrogenases.

Results

The in vitro system to study [NiFe]-hydrogenase maturation

The anoxic reaction mixture was composed of purified HybC, the core maturation complex HybG–HypDE (GDE), purified accessory proteins ^{His}HypE and ^{His}HypF in stoichiometric amounts, and an activation mix including ATP, carbamoyl phosphate, $NiCl_2$, $FeSO_4$, and sodium dithionite. The reaction was started by the addition of endopeptidase HybD in catalytic amounts. After 30 min of incubation time at room temperature, aliquots of the reaction mixture were analyzed by SDS-PAGE for cleavage of HybC (~63.5 kDa) into the processed form, $HybC^{-15AA}$ (~62 kDa) (Fig. 2*A*). Maximal cleavage was observed for the complete reaction mix (*lane 1*). Although HypE is supplied to the reaction mix in the form of the GDE complex, without the addition of extra ^{His}HypE (*lane 2*) to the reaction assay, only ~60% cleavage was detected. The cleavage of ~20% of HybC in the absence of ^{His}HypF (*lane 3*) can be explained by the presence of $Fe(CN)_2CO$ on the GDE complex (14). Notably, the maximal cleavage shown in *lane 1* was achieved by the addition of equimolar ratio of purified ^{His}HypE and ^{His}HypF to the reaction mix, and if either component of HypE or HypF is missing from reaction assay, the counterpart component cannot stimulate the maturation reaction. No cleavage of HybC could be observed when the reaction was performed in the absence of the GDE complex (*lane 4*), HybD endopeptidase (*lane 5*), or activation mix (*lane 6*) or under aerobic conditions (*lane 7*). No significant increase in cleavage after 60 min of incubation was observed. For longer incubation times, a decrease of enzyme activity was observed, potentially

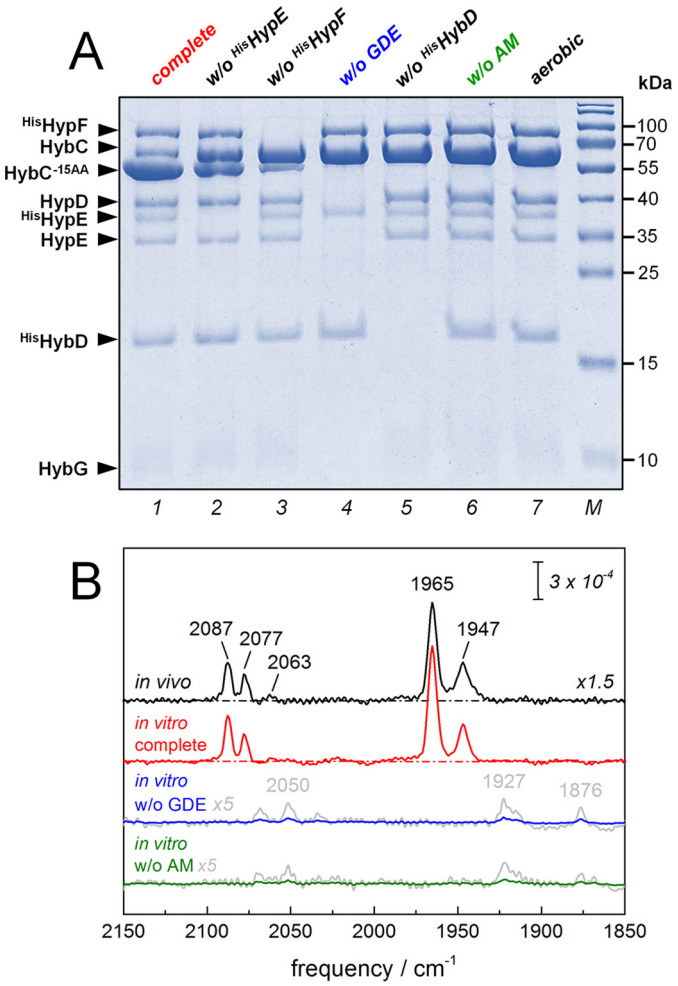

Figure 2. *In vitro* system to study the maturation of [NiFe]-hydrogenase 2 from *E. coli*. *A*, SDS-PAGE analysis of the *in vitro* assay. The complete assay was composed of purified HybC; accessory proteins HybG–HypDE complex (GDE), ^{His}HypE, and ^{His}HypF; the endopeptidase ^{His}HybD; and the AM. After 30 min of incubation, aliquots of reaction mixture were analyzed for cleavage of HybC by SDS-PAGE. The complete assay in *lane 1* predominantly showed cleavage of HybC (~63.5 kDa) into HybC^{-15AA} (~62 kDa). Approximately 60 and 20% cleavage activity was observed in the absence of ^{His}HypE and ^{His}HypF, respectively (*lanes 2* and *3*). Note the visible presence of native HypE in *lane 2*, which originates from the GDE. In the absence of the HybG–HypDE complex (without (*w/o*) GDE), endopeptidase HybD (*w/o HybD*), or the activation mixture (*w/o AM*), no cleavage was observed (*lanes 4–6*). *Lane 7* shows that aerobiosis disrupted cleavage as well. *B*, FTIR analysis of the CO/CN vibrational fingerprint of the cofactor. Both *in vivo* (*black*) and *in vitro* (*complete*, *red*) matured hydrogenase-2 signatures were identical and comprised two redox species at least (CN frequencies 2087, 2077, and 2063 cm^{-1}; CO frequencies 1965 and 1947 cm^{-1}). Efficiently, no formation of cofactor was observed in the absence of the HybG–HypDE complex (*in vitro w/o GDE*, *blue*) or activation mixture (*in vitro w/o AM*, *green*). Only residual traces of CO/CN bands can be observed (*gray*, magnified ×5).

due to protein degradations that appear as a smear on SDS-PAGE rather than separate bands (data not shown). Infrared spectroscopy showed the CO/CN vibrational fingerprint of the cofactor for *in vitro* (complete) and *in vivo* matured hydrogenase-2 (Fig. 2*B*). The presence of two CO bands suggested co-population of two redox species (18, 19). We tentatively assign these peaks to the "activated" Ni-C and fully reduced Ni-R state (1965 and 1947 cm^{-1}, respectively). Both Ni-C and Ni-R are reported to be involved in the catalytic cycle of [NiFe]-hydrogenase (7). In the absence of maturation proteins (GDE) or activation mix (AM), no formation of cofactor was observed (Fig. 2*B*). However, upon closer inspection, traces of putative CO/CN bands at lower wave numbers were detected.

Analysis of hydrogenase-2 activity matured in vitro

Although HybC potentially harbors a [NiFe]-center, the large subunit alone does not exhibit hydrogenase activity. The presence of hydrogenase-2 small subunit HybO is required for enzyme activity (16). After maturation of HybC as described above, we therefore added a fraction of enriched HybO to HybC and analyzed for hydrogen conversion activity by ATR FTIR spectroscopy. Here, *in vitro* (complete) matured hydrogenase-2 was reduced by deuterium gas (D_2), and the release of deuterium ions into the H_2O bulk was followed in real time (Fig. 3*A*). Recombination of D^+ and OH^- ions gave rise to intense bands at 2505 and 1445 cm^{-1} that can be assigned to semi-heavy water (O–D stretch and HDO bending, respectively). These bands are a highly specific marker for hydrogen uptake activity. See the legend to Fig. 3 for further details on the observed difference spectrum, which also comprises spectral features of film swelling. Fig. 3*B* shows comparable activity of hydrogenase-2 matured *in vivo*. In the absence of the GDE complex or AM, hydrogenase-2 was limited to residual D_2 oxidation activity. The D_2-minus-N_2 difference spectrum of *in vitro* maturated hydrogenase-2 shows cofactor reduction upon D_2 uptake (Fig. 3*B*, *inset*). At least three reduced species in the fingerprint region of the cofactor were populated (CO bands 1951, 1936, and 1927 cm^{-1}), and a similar red shift was observed in the CN region (2075 and 2063 cm^{-1}). Future work will identify the involved redox species in greater detail. Additionally, the samples were analyzed for H_2 uptake activity by following hydrogenase-dependent reduction of benzyl viologen photometrically (Fig. 3*C*). The specific activity of purified *in vivo* maturated hydrogenase-2 was 1.88 ± 0.11 μmol of H_2 oxidized/min/mg. This value represents 100% activation and serves as an estimate of the maximum hydrogenase-2 activity that can be restored *in vitro*. Under the same reaction conditions, the highest activity obtained was in the presence of all components of the *in vitro* assay (Fig. 3*C*, *complete*). Without the addition of an equimolar ratio of ^{His}HypE and ^{His}HypF to the reaction mix, only ~70 and ~30% of enzyme activity could be restored, respectively. Only background activity that varied between an undetectable level and 6.8% of maximal activity was observed when GDE, HybD, HybO, or AM was omitted. The background activity is most probably due to nonspecific assembly of cofactor in trace amounts (compare Fig. 2*B*). HybO alone shows no hydrogenase activity. Furthermore, incubation performed under aerobic conditions completely abolished H_2 uptake activity.

The C-terminal peptide on HybC is essential for interaction with the hydrogenase maturation machinery

HybC is known to form a stable complex with the accessory protein HybG (20). HybG and HypD are the core complex of the hydrogenase-2 maturation machinery. With our *in vitro* system, we addressed the question of whether the 15-amino acid C-terminal extension on HybC is required for interaction with the HybG protein. Complex formation of Strep-tagged HybG with HybC, HybC^{-15AA}, or HybC^{+5AA} was investigated.

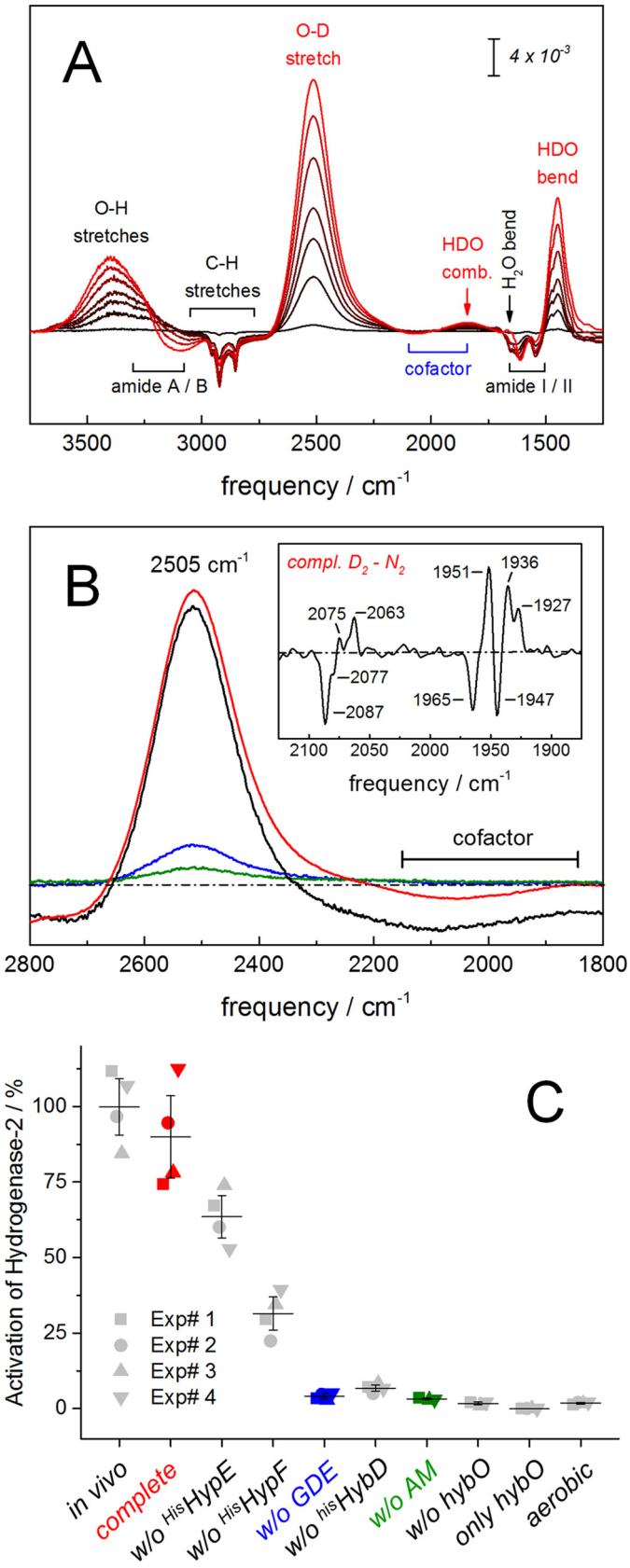

Figure 3. Analysis of hydrogenase activity matured *in vitro*. *A*, FTIR analysis of oxidation activity of *in vitro* maturated hydrogenase-2 in the presence of H_2O and D_2. Catalytic activity is followed via D_2 oxidation and release of deuterium ions into the H_2O bulk. This induces a hydrogenase-specific increase of HDO (bands at 2505, 1850, and 1445 cm^{-1}; *red labels*). Further signals show a slight increase of liquid water (O–H stretches at 3400 cm^{-1} and H_2O bending around 1660 cm^{-1}) and a concomitant decrease of protein bands (*i.e.* CH stretches from 3000 to 2750 cm^{-1}, amide I/II vibrations from 1650 to 1500 cm^{-1}, and a decrease of N–H stretches from 3300 to 3100 cm^{-1} (amide A/B) (60). *B*, matured hydrogenase-2 as isolated (*in vivo*, *black*) or as synthesized *in vitro* (*in vitro complete*, *red*) did not differ significantly in D_2 uptake activity. Residual activity was observed in the absence of the HybG–HypDE complex (*in vitro w/o GDE*, *blue*) or activation mixture (*in vitro w/o AM*, *green*). Note the D_2-N_2 difference spectrum of *in vitro* synthesized hydrogenase-2 (*inset*). Here, the population of at least three reduced species is shown (positive CO frequencies at 1951, 1936, and 1927 cm^{-1}). *C*, kinetic analysis of H_2 uptake activity. The complete assay was composed of purified HybC, GDE, HypE, HypF, the endopeptidase HybD, HybO, and AM. Reactions were conducted in the absence of one or more substrates at a time, as indicated. The samples were analyzed for activity by following H_2-dependent reduction of benzyl viologen photometrically under the same reaction conditions. The specific activity of purified hydrogenase-2 (*in vivo*) was 1.88 μmol of H_2 oxidized/min/mg. This activity represents 100% activation and provides an estimate of the maximum activity expected for the *in vitro* matured hydrogenase. The maximal attainable activity obtained under this condition was in the presence of all components of the *in vitro* assay (complete). Without the addition of an equimolar ratio of ^{His}HypE and ^{His}HypF to the reaction mix, ~70 or 30% of enzyme activity could be restored, respectively. Only background activity was observed when GDE, HybD, AM, or HybO was omitted or when the incubation was performed under aerobic conditions. HybO alone shows no hydrogenase activity. Four independent experiments and the S.D. value is shown.

HybC^{-15AA} is a genetic construct equal to truncated HybC (*i.e.* without the 15 amino acids at the C terminus). HybC^{+5AA} equals HybC but includes an artificial extension of five amino acids (Gly-Leu-Cys-Gly-Arg) at the C terminus (Fig. 4*A*).

The plasmid p-hybG was expressed together with either p-hybC or p-hybC^{-15AA} plasmid in the strain FTD-G (Table 2). The respective cell extracts were subjected to chromatography on a Strep-Tactin affinity column. The result shows that HybG interacted exclusively with HybC but not with the truncated variant HybC^{-15AA} (Fig. 4*B*). Furthermore, we addressed the question of whether the C-terminal extension on HybC is important for recruitment of other proteins involved in maturation. To probe this, the plasmid pT-hybG^{Strep}-hypDEF was expressed together with either HybC^{-15AA}, HybC, or HybC^{+5AA}. Analysis of the isolated protein complexes after Strep-Tactin affinity chromatography revealed that only HybC interacted with the core complex HybG–HypD, whereas both HybC^{-15AA} and HybC^{+5AA} did not interact (Fig. 4*C*, *lanes 1–3*). To determine whether HypE and/or HypF are required for HybG and HypD to form a complex with HybC, the experiment was repeated in a *hypF* or *hypE* deletion background. The plasmid pT-hybG-hypDE was expressed into *hypF* deletion strain FTD-F, whereas plasmid pT-hybG-hypDF was expressed in the *hypE* deletion strain FTD-E. The lack of HypF or HypE (Fig. 4*C*, *lanes 4–6* (Δ*hypF*) and *lanes 7–9* (Δ*hypE*)) appeared to have no negative impact on the ability of HybC to interact with the HybG–HypD core complex (Fig. 4*C*, *lanes 5* and *8*). Our study also demonstrates that extension of the C terminus by five amino acids (HybC^{+5AA}) prevents interaction with HybG–HybD (Fig. 4*C*, *lanes 1*, *4*, and *7*). Altogether, these results indicated that the C-terminal extension on HybC is important for interaction with HybG–HypD of the maturation machinery. HybG and HypD form the central maturation complex, with neither HypE nor HypF being essential for complex formation with HybC.

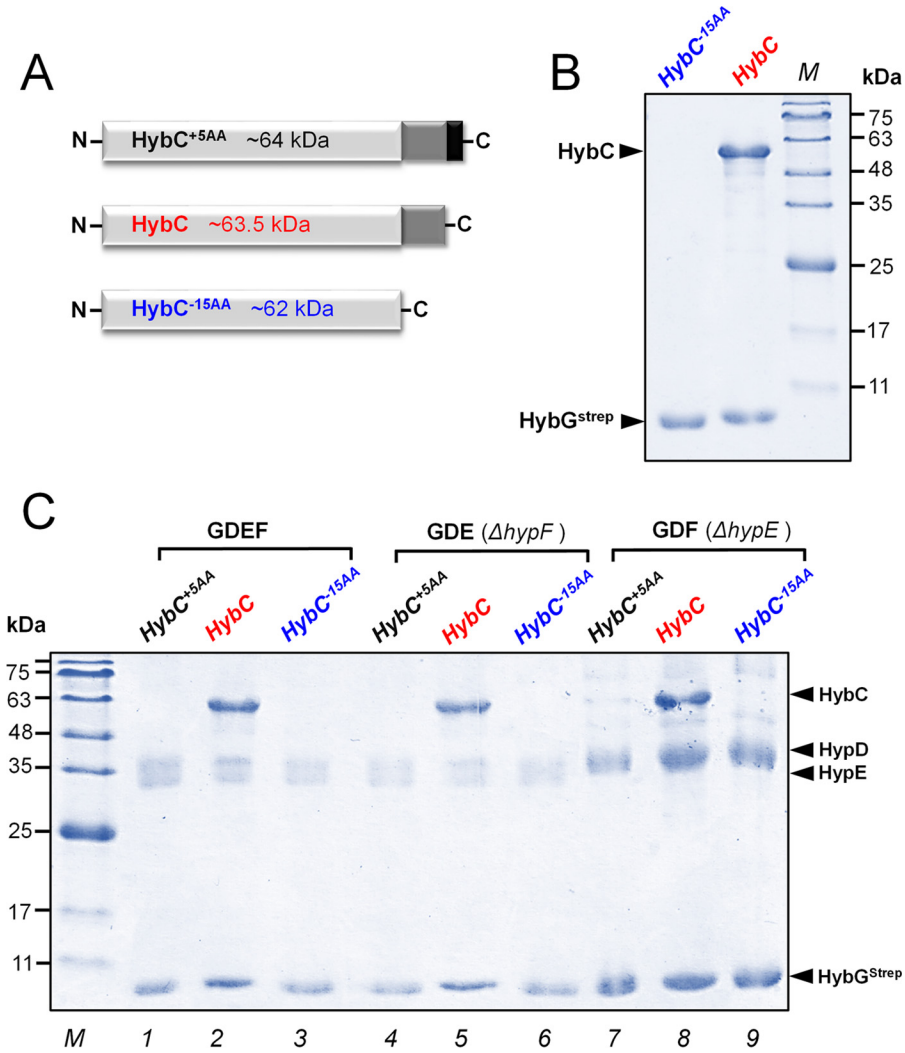

Figure 4. Interaction of HybC variants with maturation proteins HybG^{Strep} and HypDEF. *A*, schematic representation of HybC^{+5AA} (*black*), HybC (*red*), and HybC^{-15AA} (*blue*). HybC^{+5AA} is a genetic construct with an additional five amino acids at the C terminus. The HybC^{-15AA} variant lacks the C-terminal extension. *B*, the respective proteins were overproduced in *E. coli*, and subsequently HybG^{Strep} was pulled out from the cell extracts by Strep-Tactin affinity chromatography. Shown is SDS-PAGE analysis of complexes HybG^{Strep} and HybC^{-15AA} (*lane 1*) or HybG^{Strep} and HybC (*lane 2*). Note that HybC but not HybC^{-15AA} forms a complex with HybG^{Strep}. *C*, SDS-PAGE analysis of 20 μg of HybG^{Strep} complexes pulled out of extracts containing overproduced HybG^{Strep}–HypDEF(GDEF) and either overproduced HybC^{+5AA} or HybC or HybC^{-15AA} (*lanes 1–3*). The experiment was repeated with extracts, in which either HypF (GDE Δ*hypF*; *lanes 4–6*) or HypE (GDF Δ*hypE*; *lanes 7–9*) was lacking. Again, only HybC formed a complex with HypG^{Strep}. HypF and HypE were found to be not essential for the interaction of HybG^{Strep} and HybC (*lanes 5* and *8*).

Cleavage of the C-terminal peptide on HybC after cofactor assembly is essential for the formation of active hydrogenase

We investigated at which stage during maturation the C-terminal extension of HybC is cleaved off. The individual compositions of protein complexes of the *in vitro* assays were analyzed at different maturation steps by SDS-PAGE (Fig. 5*A*). *Lane 1* shows the complete reaction mix but lacking HybD endopeptidase. The reaction was started by the addition of HybD, and immediately afterward, an aliquot was analyzed (*lane 2*, t_0). No HybC^{-15AA} was detected. After t = 10, 20, and 30 min of incubation at room temperature, HybC^{-15AA} was observed in increasing amounts (*lanes 3–5*). No additional processing of HybC after 20 min was observed. Both unprocessed ^{Strep}HybC and processed ^{Strep}HybC^{-15AA} were isolated from the reaction mix by Strep-Tactin affinity chromatography (*lane 6*). Fig. 5*B* shows SDS-PAGE analysis of an enriched ^{His}HybO fraction (*lane 1*). The ^{His}HybO fraction was added to a fraction containing ^{Strep}HybC and ^{Strep}HybC^{-15AA} (*lane 2*). Subsequently, active holoenzyme ^{Strep}HybC–^{His}HybO was isolated by histidine affinity chromatography (*lane 3*). These results demonstrate that the processed ^{Strep}HybC^{-15AA}, but not the unprocessed HybC protein, forms a heterodimer with the small subunit HybO. Removal of the C-terminal extension appears to be a prerequisite for formation of catalytically active [NiFe]-hydrogenase.

To determine whether the C-terminal extension of HybC is required for synthesis of active hydrogenase also *in vivo*, plasmids encoding either N-terminal His-tagged HybC or equally tagged HybC^{-15AA} were introduced into a *hybC* deletion strain of *E. coli* (21). After anaerobic growth, recombinant HybC and HybC^{-15AA} proteins were isolated by histidine affinity chromatography (Co^{2+}-charged resin). The HybC preparation exhibited hydrogenase activity (Fig. 3, *B* and *C*; *in vivo*) and showed the $(CN)_2CO$ signature of a [NiFe]-center (Fig. 2*B*; *in vivo*), but

Table 2
Strains and plasmids used in this study

Strains/plasmids	Genotype	Source/Reference
Strain		
MC4100	F$^-$ *araD139* α *(argF-lac)U169 ptsF25 deoC1 relA1 flbB5301 rspL150*$^-$	Ref. 58
BL21(DE3)	F-ompT hsdSB (rB-,mB-)gal dcm (DE3)	Novagen
FTD147	MC4100 Δ*hyaB* Δ*hybC* Δ*hycE*	Ref. 21
FTD-F	MC4100 Δ*hyaB* Δ*hybC* Δ*hypF*::*Kan*^{R}	This study
FTD-E	MC4100 Δ*hyaB* Δ*hybC* Δ*hypE*::*Kan*^{R}	This study
FTD-G	MC4100 Δ*hyaB* Δ*hybC* Δ*hycE* Δ*hybG*::*Kan*^{R}	This study
FTD-O	MC4100 Δ*hyaB* Δ*hybC* Δ*hycE* Δ*hybO*::*Kan*^{R}	Ref. 16
Plasmid		
pT-hybG-hypDEF	pT7-7, *hypD*, *hypE*, his-TEV-*hybG*, *hypF*, km^R	This study
pT-hybG-hypDEF	pT7-7, *hypD*, *hypE*, *hybG*-Strep, *hypF*, Amp^R	This study
pT-hybG-hypDE	pT7-7, *hypD*, *hypE*, *hybG*-Strep, Amp^R	This study
pT-hybG-hypDF	pT7-7, *hypD*, *hybG*-Strep, *hypF*, Amp^R	This study
p-hypF	pET28A, *hypF*, encodes His-HypF, km^R	Ref. 39
p-hypE	pET28A, hypE, encodes His-HypE, km^R	Ref. 39
pC-hybO	pET28A, hybO, encodes His-HybO, km^R	This study
pC-hybD	pCA24N, hybD, encodes His-HybD	This study
p-hybC^{+5AA}	pCA24N, hybC, encodes His-HybC^{+5AA} (GLCGR), Cm^R	Ref. 59
p-hybC	Like p-hybC^{+5AA} but with a stop codon, which removes the codons encoding GLCGR	Ref. 32
p-hybC^{-15AA}	Like p-HybC but a stop codon at position encoding codon V553, which removes the 15-amino acid C-terminal peptide	This study
pASK-HybC	pASK-IBA5, hybC, encodes Strep-HybC, Amp^R	Ref. 39
p-hybG	pASK-IBA3, encodes hybG-Strep, Amp^R	Ref. 27

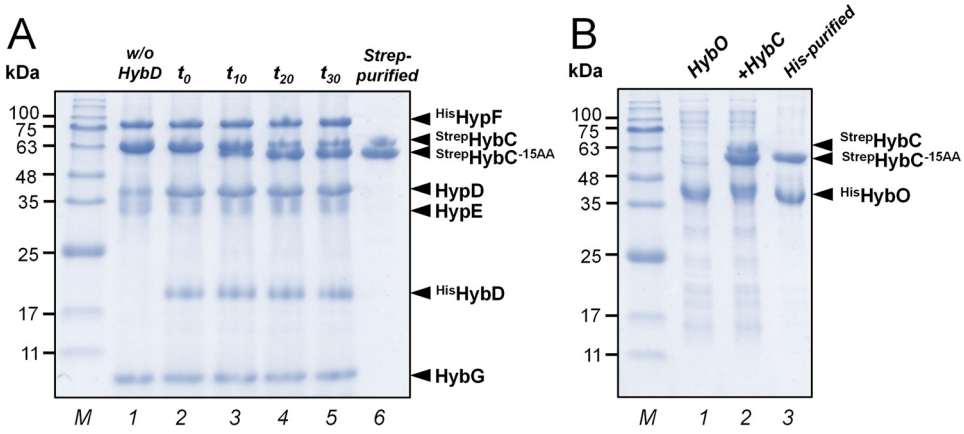

Figure 5. SDS-PAGE analysis of protein compositions of *in vitro* assays at different maturation steps. *A*, *in vitro* processing of hydrogenase-2 catalytic subunit HybC. *Lane 1*, reaction mix contained HybC, GDE complex, HypE, and HypF in stoichiometric amounts (2 μM each) and AM. *Lane 2*, the reaction was started by the addition of endopeptidase HybD in catalytic amounts, and immediately an aliquot of the reaction mix (~25 μg) was analyzed (t_0). No HybC^{-15AA} was detected. *Lanes 3–5*, aliquots of the reaction mix were analyzed after 10, 20, and 30 min of incubation at room temperature, respectively (t_{10}, t_{20}, and t_{30}). HybC^{-15AA} formation was observed over time. After 20 min, no additional processing of HybC was observed. *Lane 6*, isolation of both unprocessed ^{Strep}HybC and processed ^{Strep}HybC^{-15AA} from the reaction mix by Strep-Tactin affinity chromatography. *B*, formation of HybC–HybO holoenzyme. *Lane 1*, ^{His}HybO-enriched fraction. *Lane 2*, the ^{Strep}HybC and ^{Strep}HybC^{-15AA} fraction isolated from reaction mix was supplemented with the ^{His}HybO-enriched fraction. *Lane 3*, the ^{Strep}HybC–^{His}HybO heterocomplex was isolated by a histidine affinity column. Only the processed large subunit (HybC^{-15AA}) can form a heterodimer with the small subunit HybO.

the HybC^{-15AA} preparation was inactive and devoid of cofactor (data not shown). These results support the aforementioned findings that truncated HybC (HybC^{-15AA}) is not able to recruit the hydrogenase maturation machinery and thus hinders maturation into active enzyme also *in vivo*.

Conformational changes of HybC upon removal of the C-terminal peptide

To detect possible conformational changes associated with cleavage of pro-protein, we purified and analyzed HybC, HybC^{-15AA}, and HybC^{+5AA} by CD and native gradient gel electrophoresis. Far-UV CD spectroscopy (150–250 nm) is sensitive to changes in secondary structure of proteins, whereas near-UV CD (250–350 nm) monitors alterations in the environment of aromatic amino acid side chains (*i.e.* changes in the tertiary structure of proteins) (22–24). Notably, the C-terminal extension does not contain any aromatic amino acids. Spectra of HybC (*red*) and HybC^{+5AA} (*black*) were found to be almost identical (Fig. 6). Thus, the five-amino acid extension of the C terminus of HybC does not lead to structural changes in the protein. In contrast, the truncated HybC^{-15AA} protein showed significant spectral differences in far- and near-UV CD spectroscopy (Fig. 6, *A* and *B*). Changes of far CD spectra are probably due to differences in the content of regular secondary structural features, such as the α-helix and β-sheet. Near-CD spectra indicate changes in the environment of aromatic amino acid side chains (*e.g.* changes in tertiary structure of the protein after removal of the C-terminal extension). Native PAGE (Fig. 6*C*, *left*) showed clear changes in migration behavior of HybC after removal of the C-terminal extension. The five-amino acid extension of HybC did not lead to changes in migration behavior, because both HybC^{+5AA} and HybC migrated faster and

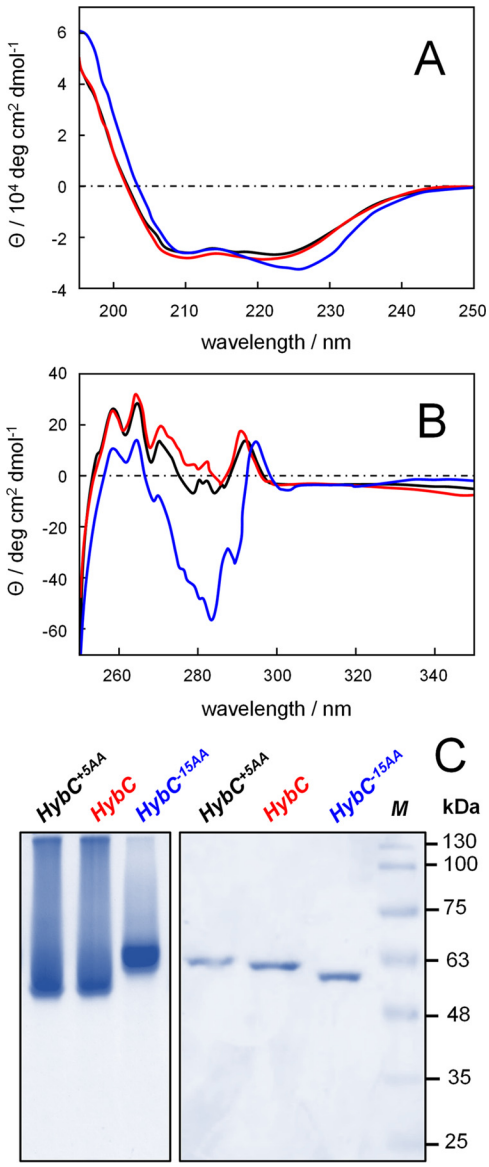

Figure 6. Conformational changes of HybC upon removal of the C-terminal peptide. *A*, far-UV CD spectra; *B*, near-UV CD spectra of HybC^{+5AA} (*black*), HybC (*red*), and HybC^{-15AA} (*blue*). The five-amino acid extension on HybC does not lead to significant conformational changes. In contrast, removal of the C-terminal extension induces clear conformational changes in secondary and tertiary structure (compare *red* and *black versus blue*). *C*, native PAGE analysis (*left*) shows clear changes in migration behavior after removal of the C-terminal extension. The HybC^{-15AA} protein band is sharper and migrates slower than HybC and HybC^{+5AA} variants, indicative of a different conformation. SDS-PAGE (*right*) reveals the only small differences in mass between HybC variants.

showed broad, diffuse protein bands. In contrast, upon removal of C-terminal extension, the HybC^{-15AA} migrated slower and showed a sharper protein band. SDS-PAGE was used to resolve and confirm the small differences in mass between HybC variants (Fig. 6*C*). In sum, these results indicate that conformational changes in secondary and tertiary structure of HybC take place upon removal of C-terminal extension.

Discussion

Maturation of [NiFe]-hydrogenases *in vitro* provides the possibility to prove and refine our understanding of [NiFe]-cofactor biosynthesis. The presented approach exclusively relies on purified components and allows studying the order of events individually. Our maturation assay included HypE and HypF, both of which have been shown to synthesize the CN ligands from carbamoyl phosphate, as supplied with the activation mixture (25, 26). Although HypE and HypF are absolutely required for synthesis of the cyano-ligands, partial cleavage of HybC took place in their absence. This is due to the presence of HypE that was supplied to the reaction mix in the form of the GDE complex. The reason for cleavage in the absence of HypF is the presence of $Fe(CN)_2CO$ on the GDE complex that allows for partial assembly of [NiFe]-cofactor (14). Only the complete assay, including HypE and HypF, allows for multiple maturation turnover, as supported by formation of [NiFe]-cofactor and maturation of hydrogenase-2 *in vitro* at activity levels near those of the *in vivo* matured enzyme. Lenz and co-workers (61) recently identified the accessory protein HypX that synthesizes the CO ligand of O_2-tolerant [NiFe]-hydrogenases from formyl-tetrahydrofolate. However, the anaerobic route of biosynthesis remains ambiguous because *E. coli* lacks HypX or orthologue enzymes (27).

An interesting aspect of performing *in vitro* reconstitution with purified proteins is whether a particular protein has a direct participation in the maturation process or not and which minimal combination of components is sufficient to achieve complete maturation. This capability provides a rapid means of "quality control" with regard to the reproducibility of the purification procedures for the individual enzymes by confirming the activity of the purified proteins individually. The functionality of the purified GDE complex, HypE, HypF, HybD, HybC, and HybO was confirmed by activity measurements of maturation assays complemented with the corresponding missing protein, as shown in Fig. 3*C*. FTIR analysis performed in previous and current studies indicates that anaerobically purified GDE complex carries two cyano-ligands, one CO ligand and bound CO_2 (14). Whereas HypD alone shows infrared bands assigned to one CO and two CN ligands (28), purified HybG exhibits a band characteristic of bound CO_2 (27). Metal analysis determined by inductively coupled plasma mass spectrometry (ICP-MS) showed that the GDE complex contained ~4.4 iron ions/mol of ternary complex, whereas HybG contained substoichiometric amounts of iron (~0.3 mol of iron/mol of HybG). The amount of nickel, copper, cobalt, and zinc was below the detection limit (14). Employing the GDE complex that does not harbor the $Fe(CN)_2CO$ moiety could not restore hydrogenase activity. Therefore, the presence of the $Fe(CN)_2CO$ moiety seems to be necessary for hydrogenase-2 maturation *in vitro*. No hydrogenase activity could be measured when the GDE complex was replaced by HybG, HypD, or HypE individually or in combination after separate purification (14). This finding indicates that the physical ternary complex carrying the $Fe(CN)_2CO$ moiety is essential for successful activation of hydrogenase-2. Anerobically purified HypD protein preparations typically contain five equivalents of iron and four sulfides per protein molecule (28). Four of these iron ions are associated with a low-potential [4Fe-4S] cluster (29). Electron paramagnetic resonance (EPR) and Mossbauer spectroscopy on HypD revealed a diamagnetic $[4Fe\text{-}4S]^{2+}$ cluster (30). The fifth iron

ion was proposed to coordinate the $(CN)_2CO$ ligands (28). HypD is the only Hyp [4Fe-4S] cluster containing protein and is therefore likely to be capable of performing redox chemistry and delivering electrons for CO and CN ligand generation (29). During the course of this study, HypD was found to catalyze the CO-dependent reduction of the electron acceptor methyl viologen with a maximal rate of 24 milliunits/mg of protein. However, the reverse reaction, CO_2-dependent oxidation of reduced methyl viologen, performed in the presence of ATP could not be observed (data not shown). Analysis of anaerobically purified HypF revealed that the protein contained only substoichiometric amounts of iron and zinc (~0.1 mol of iron and 0.4 mol of zinc per HypF monomer). The UV-visible spectrum did not indicate the presence of any cofactor. Similar results were obtained for the aerobically purified HypF (26). The carbamoyl phosphate phosphatase activity of HypF was routinely confirmed by the release of inorganic phosphate directly in non-denaturing polyacrylamide gels (31). The functionality of purified HypE and HypF was also routinely verified by observation of the cyanation on HypE from carbamoyl phosphate in an ATP-dependent condensation reaction using ATR FTIR (25). The addition of only HypF or HypE to the reconstitution reaction had no effect on the level of hydrogenase activity, but the addition of both (complete reaction) increased the hydrogenase activity about 2-fold. This suggests that an equimolar ratio of HypE and HypF is needed for full reconstitution of hydrogenase activity. Anerobically purified HybC precursor isolated from any hydrogenase deletion mutant of *hypF*, *hypE*, *hypD*, or *hybD* was unprocessed, was not associated with the small subunit HybO, and lacked enzyme activity. These HybC preparations were colorless and lacked cofactor or any associated metal, as indicated by UV-visible spectrum and ICP-MS analysis. In a Hyp-competent genetic background, the HybC precursor can be matured *in vivo* and *in vitro* and delivers active hydrogenase-2. In contrast, the isolated $HybC^{+5AA}$ could not be matured, was brown, and had substoichiometric amounts of an oxygen-sensitive iron–sulfur cluster (0.2 mol of iron/mol of $HybC^{+5AA}$). This cluster is coordinated by the conserved cysteinyl residues that normally ligate the $NiFe(CN)_2CO$ cofactor, as was shown by UV-visible spectroscopy and EPR (32).

Isolation of the small subunit HybO in its active form was more challenging. The pC-hybO plasmid that encodes for N-terminal His-tagged protein (^{His}HybO) was transformed in *E. coli* strain FTD-O, which lacks the genes encoding HybO and the large subunit of hydrogenase-2 (Table 2). Overproduction and purification of ^{His}HybO was not possible due to inclusion body formation. A low level of soluble protein without isopropyl 1-thio-β-D-galactopyranoside induction (~0.70 mg of protein per 5 g wet weight of anaerobically grown cells) could be isolated by histidine affinity chromatography, but ^{His}HybO was labile due to the imidazole-containing elution buffer and could not restore hydrogenase activity *in vitro*. We therefore separated the soluble fraction containing ^{His}HybO by ultracentrifugation and subsequent ion-exchange chromatography. The ^{His}HybO fraction was brown and most likely present as holoprotein with three iron–sulfur clusters. It should be noted that the HybO protein concentration in hydrogenase deletion mutants was usually at a low level, particularly if the large subunit is absent (17). This can be due to rapid turnover of HybO. These results suggest that direct physical contact between the large and small subunit is required to ensure stability of the small subunit against degradation.

The results provide evidence that the C-terminal extension of the large subunit HybC is removed only after cofactor assembly and before complex formation with the small subunit HybO has occurred. Proteolytic cleavage is thus a checkpoint that guarantees formation of catalytically active [NiFe]-hydrogenase exclusively. The underlying mechanism was shown to be a larger conformational change associated with removal of the 15 C-terminal amino acids. We suggest that proteolytic cleavage of HybC triggers structural changes and induces formation of the [NiFe]-center from the $Fe(CN)_2CO$ moiety and nickel (33). It has been hypothesized that changes in conformation precede the internalization of the metal center within the large subunit (5). Crystal structures show that the [NiFe]-cofactor lies close to the interface with the small subunit (34).

The data presented in this study suggest that the role of the C-terminal extension is maintaining a "correct" conformation of the HybC protein that facilitates interaction with accessory proteins HybG–HypDEF. We could demonstrate that maturation proteins, particularly HybG, interact specifically with HybC but are incapable of interacting with truncated $HybC^{-15AA}$. Most likely, the different conformation adopted by $HybC^{-15AA}$ prevents the interaction. During synthesis of hydrogenase-3, HypC (a homologue of HybG) forms a stable complex with the pro-protein of the large subunit of hydrogenase-3. This complex was found to accumulate in mutants unable to synthesize the $NiFe(CN)_2CO$ cofactor (35). Therefore, it is likely that complex formation between the unprocessed large subunit and the hydrogenase maturation machinery makes HybC accessible for the incoming cofactor (5). Because we observe formation of the HybC–HybO heterodimer exclusively with processed HybC, it seems that the C-terminal extension on HybC prevents complex formation with HybO. Upon removal of the C-terminal peptide, far-CD spectroscopy indicates rather insignificant conformational changes in secondary structure. In contrast, global changes in tertiary structure of the protein are suggested by the observed difference in the near-UV spectra between HybC and $HybC^{-15AA}$. This difference is most likely due to the tertiary folding of the polypeptide chain, which can place the aromatic amino acid side chains in chiral environments, thus giving rise to circular dichroism (22, 24). This is in good agreement with the proposed refolding of HybC upon cleavage of the C-terminal peptide (5). The fully folded and cofactor-containing HybC large subunit can then engage with the small subunit to form catalytically active heterodimer. This would ensure that in wild-type cells, only a large subunit with a complete [NiFe]-cofactor proceeds along the maturation path. A similar function was suggested for the C-terminal extension of hydrogenase-3 of *E. coli* and the membrane-bound [NiFe]-hydrogenase of *Ralstonia eutropha* (36, 37).

Biosynthesis and insertion of [NiFe]-cofactor involves a multistep pathway catalyzed by different compositions of accessory proteins (20, 38). Precursors of [NiFe]-hydrogenase are unsta-

ble in aqueous solutions and highly sensitive to oxygen (39, 40); thus, it seems likely that accessory and pro-protein form a supramolecular complex during maturation. A stable "supercomplex" consisting of HybG, HypD, HypE, and HybC was isolated in this work. Furthermore, multiprotein complexes containing HypA, HypB, SlyD, and pro-protein of hydrogenase-3 were observed earlier (49).

The C-terminal extension of the large subunit varies greatly both in sequence and length among different hydrogenases and organisms. Intriguingly, there are examples of hydrogenases whose large subunit lacks a C-terminal extension including H_2-sensory and energy-converting [NiFe]-hydrogenases (41, 42). During the course of this study, the large subunit of [NiFe]-hydrogenase from *Carboxydothermus hydrogenoformans* (CooH) or *Thermoanaerobacter tengcongensis* (EchE), in which the C-terminal extension is missing (43, 44), could not be synthesized in an active form in *E. coli*. In reciprocal heterologous complementation studies, anaerobically purified heterologous HybG–HypDE complex, where HypD was replaced by HypD either from *C. hydrogenoformans* or from *T. tengcongensis*, was not capable of assembling and maturing active hydrogenase-2 in *E. coli* (data not shown). How insertion of the [NiFe]-cofactor and subunit assembly are coordinated in these enzymes remains to be investigated. However, it is possible that the hydrogenase-specific maturation machinery in these organisms encodes for a peptide that functionally replaces the C-terminal extension. In support of this is the finding that the extension must not be covalently linked to the large subunit but can be part of a separate polypeptide (45).

In conclusion, this study highlights the role of the C-terminal extension on the hydrogenase catalytic subunit. The 15-amino acid peptide promotes the complete sequence of maturation events by directing and binding maturation proteins and ensuring that only the cofactor-containing large subunit can continue on the assembly line toward active [NiFe]-hydrogenase.

Experimental procedures

Bacterial strains and growth conditions

All *E. coli* strains and plasmids used are listed in Table 2. Strains were generally grown anaerobically in LB or in modified TB medium. The antibiotics kanamycin, chloramphenicol, and ampicillin were added to the medium at final concentrations of 50, 15, and 100 μg/ml respectively. For overproduction of proteins, *E. coli* strains, BL21(DE) (46), FTD147 (21), or the indicated strains were transformed with the appropriate plasmid and grown anaerobically in modified TB medium at 37 °C until the optical density at 600 nm (A_{600}) reached 0.3. Gene expression was induced by the addition of 0.2 μg/ml anhydrotetracycline or 150 μM isopropyl 1-thio-β-D-galactopyranoside followed by incubation at 30 °C for 3–5 h or after the culture reached an optical density at 600 nm between 0.7 and 0.9 (exponential phase cultures). Cells were harvested by centrifugation at 10,000 × *g* for 15 min at 4 °C. Large-scale protein purification was performed with 20 liters of anaerobic TB medium (3–4 g of cells/liter culture).

Strain and plasmid construction

Strains were constructed by the introduction of mutations from *E. coli* donor strains into recipient strains of MC4100 derivatives by P1*kc*-mediated phage transduction. Plasmid p-hybC served as DNA template for the introduction of mutation into the *hybC* gene using the QuikChange site-directed mutagenesis strategy of Stratagene. The oligonucleotide primers used to introduce a stop codon at position Val-553 of HybC were 5′-GCCTGTGCGGTACACTAAGTGGATGCTGACGGC-3′ and 5′-GCCGTCAGCATCCACTTAGTGTACCGCACAGGC-3′. To generate the pT-hybG-hypDF and pT-hybG-hypDE plasmids, the pT-hybG-hypDEF plasmid (14) was digested with BamHI or HindIII, which released either the complete *hypE* gene or the complete *hypF* gene, respectively. The p-hybG-hypDEF plasmid was used as a template for amplification of *hypD*, *hypE*, *hypF*, and *hybG* genes via PCR. The resulting PCR fragments were digested with NdeI and HindIII and ligated into NdeI-/HindIII-digested pET28A to generate the plasmid pT-hybG-hypDEF.

Preparation of crude extracts and affinity purification of protein

All steps were carried out under a nitrogen/hydrogen mixture (95:5) in an anaerobic chamber (Coy Laboratories) and at 4 °C unless stated otherwise. Cells containing Strep-tagged protein were resuspended at a ratio of 1:3 (w/v) in buffer W (100 mM Tris/HCl and 150 mM NaCl, pH 8.0) including 2 mM sodium dithionite, 5 mg/liter DNase, and 0.2 mM PMSF. Cells were disrupted by sonication (40 watts for 16 min with 0.5-s pulses). Unbroken cells and debris were removed by centrifugation for 30 min at 10,000 × *g* at 4 °C to deliver the crude extract. Three-milliliter crude extracts were applied to a 1-ml Strep-Tactin-Sepharose column (IBA Technologies) using gravity flow. Unbound proteins were removed from the column by washing with 5 column volumes of buffer W. Specifically bound proteins were eluted with buffer W including 5 mM desthiobiotin. Desthiobiotin was subsequently removed by passage through a Hi-Prep 26/10 desalting column (GE Healthcare) equilibrated with buffer W without reducing agents and connected to an ÄKTA apparatus (GE Healthcare). Proteins were concentrated by centrifugation at 5000 × *g* using centrifugal filters (Amicon Ultra, 50 K, Millipore) and stored under liquid nitrogen. His-tagged protein variants were purified from cells transformed with the appropriate plasmid derivative (Table 2). Wet cell paste was resuspended at a ratio of 1:4 (w/v) in buffer A (50 mM Tris/HCl, pH 8.0, 300 mM NaCl) including 5 mg/liter DNase and 0.2 mM PMSF. Crude extracts derived from ~10 g of wet cell paste were loaded onto a 1.5 × 10-cm column of Co^{2+}-charged resin (Talon resin, Clontech). The column, which had been previously equilibrated with buffer A, was washed with 10 column volumes of the same buffer, followed by 5 column volumes of buffer A supplemented with 10 mM imidazole and then 3 column volumes of buffer A supplemented with 20 mM imidazole to remove nonspecifically bound proteins. His-tagged proteins were subsequently eluted with buffer A containing 300 mM imidazole. Imidazole was removed by a desalting column, and proteins were concentrated as described above.

Enrichment of an active small subunit HybO required for analysis of hydrogenase activity

The pC-hybO plasmid that encodes for N-terminal His-tagged protein (^{His}HybO) was transformed in *E. coli* strain FTD-O (Table 2) and grown anaerobically in LB medium at 25 °C without induction until the optical density at 600 nm reached 0.7. The cells were disrupted by three passages through a French pressure cell. ^{His}HybO purified by histidine affinity chromatography could not restore hydrogenase activity *in vitro*. We therefore separated soluble fractions containing ^{His}HybO by ultracentrifugation at 150,000 × *g* for 2 h. Subsequently, the supernatant was loaded onto a Q-Sepharose HiLoad column, equilibrated with 100 mM Tris buffer, pH 8. The protein was eluted in a stepwise NaCl gradient. Enriched active holoprotein ^{His}HybO was recovered in the fractions eluted with 0.2 M NaCl.

The in vitro system for maturation of [NiFe]-hydrogenase-2 from E. coli

The 100-μl complete reaction mixture in 50 mM MOPS KOH, pH 7.0, contained 4 μM purified Strep-tagged HybC (39), 2 μM purified GDE complex (14), 2 μM ^{His}HypE, and 2 μM ^{His}HypF (14). An activation mix with ATP, carbamoyl phosphate, $NiCl_2$, $FeSO_4$, and sodium–dithionite was added at final concentrations of 2.5 mM, 50 μM, 100 μM, 50 μM, and 2 mM, respectively. The reaction mixtures were incubated at room temperature under nitrogen (95%) hydrogen (5%) in an anaerobic chamber. The reaction was started by the addition of a 1 μM concentration of the endopeptidase ^{His}HybD. After a 30-min incubation, 20-μl aliquots of the reaction mixture were analyzed for cleavage of HybC by SDS-PAGE using the ImageQuant software (Molecular Dynamics). Aliquots of reaction mix (80 μl) were supplemented with 0.5 mg of the small subunit HybO-enriched fraction. After 15 min, the samples were analyzed for activity photometrically.

Isolation of in vitro matured hydrogenase-2

To isolate preparative amounts of active hydrogenase-2 that was matured *in vitro*, the reaction mix was scaled up to 5 ml. Matured ^{Strep}HybC was isolated from the reaction mix by Strep-Tactin affinity chromatography. ^{Strep}HybC was supplemented with the ^{His}HybO-enriched fraction. Active ^{Strep}HybC–^{His}HybO heterocomplex was isolated by histidine affinity chromatography (Co^{2+}-charged resin). Protein samples were concentrated and analyzed by ATR FTIR as reported earlier (47).

Isolation of in vivo matured hydrogenase-2

Hydrogenase-2 was isolated from FTD-147 strain, in which a fully active enzyme was restored by introducing genes coding for HybC together with maturation proteins HybG–HypDEF on an expression plasmids pASK-hybC and pT-hybG-hypDEF. The procedure for isolating an active enzyme was according to Ref. 48.

Determination of hydrogenase activity

H_2 uptake activity was determined by following the reduction of benzyl viologen at 578 nm using an Uvicon 900 dual-wavelength spectrophotometer. The 0.8-ml assays contained 4 mM benzyl viologen in 50 mM MOPS buffer, pH 7.0. Cuvettes were allowed to equilibrate with a 100% H_2 headspace. One unit of activity corresponds to oxidation of 1 μmol of H_2/min.

Polyacrylamide gel electrophoresis

A defined amount of purified protein (3–20 μg) was separated by SDS-PAGE using 15% (w/v) polyacrylamide gels (49). Non-denaturating PAGE was performed using 7.5% (w/v) polyacrylamide gels including 0.1% (w/v) Triton X-100. Protein samples (5–100 μg) were incubated with 4% (w/v) Triton X-100 prior to application to the gels (50).

Non-heme iron and acid-labile sulfide determination

Iron and acid-labile sulfide of the GDE complex, HypD, and HybG were determined due to established protocols (51). Metal content of the GDE complex, HypD, HybG, HypE, HypF, and HybC variants was determined by ICP-MS, as described previously (32). For ICP-MS analysis, 0.1–0.2 mg of purified protein samples were analyzed for iron, nickel, zinc, cobalt, and copper.

Infrared spectroscopic characterization of HybC variants

All FTIR spectroscopy was conducted on a rapid-scan Tensor 27 spectrometer (Bruker Optik, Ettlingen, Germany) equipped with a three-reflection ZnSe/silicon crystal ATR cell (Smiths Detection, Wiesbaden Germany) as described earlier (27, 28, 47). The spectrometer was situated in an anaerobic gas chamber (Coy Laboratories, Grass Lake, MI) in a water-free atmosphere of typically 99% N_2 and 1% H_2.

Further spectroscopic characterization of HybC

Protein concentrations were determined spectroscopically using an extinction coefficient of EM (280 nm) = 97,310 M^{-1} cm^{-1}. Spectra were measured at a protein concentration of 1 mg/ml in 25 mM Tris-HCl buffer, pH 7.5, containing 150 mM NaCl using a Jasco J815 spectropolarimeter in the far-UV region (light path 0.1 mm, data accumulation 16×) and near-UV region (light path 1 cm, data accumulation 32× or 64×), respectively. For all measurements, it was ensured that the proteins were stable under the given conditions.

Quality control and metal content

No hydrogen turnover activity is associated with any of the purified maturases: GDE complex, HypE, HypF, HybD, or HybO (14, 16). Thus, catalytic competence and cofactor integrity of these enzymes had to be probed alternatively. This included the use of the maturation assay established in this study, UV-visible spectroscopy, FTIR spectroscopy, ICP-MS, and different biochemical activity assays. For example, the phosphatase activity of HypF was routinely confirmed by measuring the release of inorganic phosphate from carbamoyl phosphate (31). The specific interplay of HypE and HypF was probed by observing cyanation of HypE from inorganic phosphate in an ATP-dependent condensation reaction via surface-enhanced IR absorption spectroscopy, as established earlier (25). Furthermore, the integrity of the $Fe(CN)_2CO$ cofactor as associated with HypD and the GDE complex was routinely probed by ATR FTIR (14, 28). The presence of an iron ion and

CO_2 absorption band on HybG was confirmed by ICP-MS, UV-visible spectroscopy, and ATR FTIR (27).

Author contributions—B. S. and S. T. S. designed the research; B. S., S. T. S., and M. S. performed the research; and B. S. and S. T. S. analyzed the data and wrote the paper.

Acknowledgments—We gratefully acknowledge Rudolf Thauer for helpful discussions, Joachim Heberle and Ramona Schlesinger for ongoing support, Ute Lindenstrauss for excellent technical assistance, and Hauke Lilie for assistance with the CD spectroscopy measurements.

References

1. Waldron, K. J., and Robinson, N. J. (2009) How do bacterial cells ensure that metalloproteins get the correct metal? *Nat. Rev. Microbiol.* **7,** 25–35
2. Lu, Y., Yeung, N., Sieracki, N., and Marshall, N. M. (2009) Design of functional metalloproteins. *Nature* **460,** 855–862
3. Currin, A., Swainston, N., Day, P. J., and Kell, D. B. (2015) Synthetic biology for the directed evolution of protein biocatalysts: navigating sequence space intelligently. *Chem. Soc. Rev.* **44,** 1172–1239
4. Lill, R., and Mühlenhoff, U. (2008) Maturation of iron-sulfur proteins in eukaryotes: mechanisms, connected processes, and diseases. *Annu. Rev. Biochem.* **77,** 669–700
5. Böck, A., King, P. W., Blokesch, M., and Posewitz, M. C. (2006) Maturation of hydrogenases. *Adv. Microb. Physiol.* **51,** 1–71
6. Lacasse, M. J., Douglas, C. D., and Zamble, D. B. (2016) Mechanism of selective nickel transfer from HypB to HypA, *Escherichia coli* [NiFe]-hydrogenase accessory proteins. *Biochemistry* **55,** 6821–6831
7. Lubitz, W., Ogata, H., Rüdiger, O., and Reijerse, E. (2014) Hydrogenases. *Chem. Rev.* **114,** 4081–4148
8. Vignais, P. M., and Billoud, B. (2007) Occurrence, classification, and biological function of hydrogenases: an overview. *Chem. Rev.* **107,** 4206–4272
9. Thauer, R. K., Kaster, A. K., Goenrich, M., Schick, M., Hiromoto, T., and Shima, S. (2010) Hydrogenases from methanogenic archaea, nickel, a novel cofactor, and H-2 storage. *Annu. Rev. Biochem.* **79,** 507–536
10. Happe, R. P., Roseboom, W., Pierik, A. J., Albracht, S. P., and Bagley, K. A. (1997) Biological activation of hydrogen. *Nature* **385,** 126
11. Pierik, A. J., Roseboom, W., Happe, R. P., Bagley, K. A., and Albracht, S. P. (1999) Carbon monoxide and cyanide as intrinsic ligands to iron in the active site of [NiFe]-hydrogenases. $NiFe(CN)_2CO$, biology's way to activate H2. *J. Biol. Chem.* **274,** 3331–3337
12. Soboh, B., Stripp, S. T., Muhr, E., Granich, C., Braussemann, M., Herzberg, M., Heberle, J., and Gary Sawers, R. (2012) [NiFe]-hydrogenase maturation: isolation of a HypC-HypD complex carrying diatomic CO and CN^- ligands. *FEBS Lett.* **586,** 3882–3887
13. Watanabe, S., Kawashima, T., Nishitani, Y., Kanai, T., Wada, T., Inaba, K., Atomi, H., Imanaka, T., and Miki, K. (2015) Structural basis of a Ni acquisition cycle for [NiFe] hydrogenase by Ni-metallochaperone HypA and its enhancer. *Proc. Natl. Acad. Sci. U.S.A.* **112,** 7701–7706
14. Soboh, B., Lindenstrauss, U., Granich, C., Javed, M., Herzberg, M., Thomas, C., and Stripp, S. T. (2014) [NiFe]-hydrogenase maturation *in vitro*: analysis of the roles of the HybG and HypD accessory proteins. *Biochem. J.* **464,** 169–177
15. Theodoratou, E., Paschos, A., Magalon, A., Fritsche, E., Huber, R., and Böck, A. (2000) Nickel serves as a substrate recognition motif for the endopeptidase involved in hydrogenase maturation. *Eur. J. Biochem.* **267,** 1995–1999
16. Pinske, C., Krüger, S., Soboh, B., Ihling, C., Kuhns, M., Braussemann, M., Jaroschinsky, M., Sauer, C., Sargent, F., Sinz, A., and Sawers, R. G. (2011) Efficient electron transfer from hydrogen to benzyl viologen by the [NiFe]-hydrogenases of *Escherichia coli* is dependent on the coexpression of the iron-sulfur cluster-containing small subunit. *Arch. Microbiol.* **193,** 893–903
17. Thomas, C., Muhr, E., and Sawers, R. G. (2015) Coordination of synthesis and assembly of a modular membrane-associated [NiFe]-hydrogenase is determined by cleavage of the C-terminal peptide. *J. Bacteriol.* **197,** 2989–2998
18. Pardo, A., De Lacey, A. L., Fernández, V. M., Fan, H. J., Fan, Y., and Hall, M. B. (2006) Density functional study of the catalytic cycle of nickel-iron [NiFe] hydrogenases and the involvement of high-spin nickel(II). *J. Biol. Inorg. Chem.* **11,** 286–306
19. Ash, P. A., Hidalgo, R., and Vincent, K. A. (2017) Proton transfer in the catalytic cycle of [NiFe] hydrogenases: insight from vibrational spectroscopy. *ACS Catal.* **7,** 2471–2485
20. Butland, G., Zhang, J. W., Yang, W., Sheung, A., Wong, P., Greenblatt, J. F., Emili, A., and Zamble, D. B. (2006) Interactions of the *Escherichia coli* hydrogenase biosynthetic proteins: HybG complex formation. *FEBS Lett.* **580,** 677–681
21. Redwood, M. D., Mikheenko, I. P., Sargent, F., and Macaskie, L. E. (2008) Dissecting the roles of *Escherichia coli* hydrogenases in biohydrogen production. *FEMS Microbiol. Lett.* **278,** 48–55
22. Sreerama, N., and Woody, R. W. (2004) Computation and analysis of protein circular dichroism spectra. *Methods Enzymol.* **383,** 318–351
23. Kelly, S. M., and Price, N. C. (2000) The use of circular dichroism in the investigation of protein structure and function. *Curr. Protein Pept. Sci.* **1,** 349–384
24. Greenfield, N. J. (2006) Using circular dichroism spectra to estimate protein secondary structure. *Nat. Protoc.* **1,** 2876–2890
25. Stripp, S. T., Lindenstrauss, U., Sawers, R. G., and Soboh, B. (2015) Identification of an isothiocyanate on the HypEF complex suggests a route for efficient cyanyl-group channeling during [NiFe]-hydrogenase cofactor generation. *PLoS One* **10,** e0133118
26. Paschos, A., Bauer, A., Zimmermann, A., Zehelein, E., and Böck, A. (2002) HypF, a carbamoyl phosphate-converting enzyme involved in [NiFe] hydrogenase maturation. *J. Biol. Chem.* **277,** 49945–49951
27. Soboh, B., Stripp, S. T., Bielak, C., Lindenstrauss, U., Braussemann, M., Javaid, M., Hallensleben, M., Granich, C., Herzberg, M., Heberle, J., and Sawers, R. G. (2013) The [NiFe]-hydrogenase accessory chaperones HypC and HybG of *Escherichia coli* are iron- and carbon dioxide-binding proteins. *FEBS Lett.* **587,** 2512–2516
28. Stripp, S. T., Soboh, B., Lindenstrauss, U., Braussemann, M., Herzberg, M., Nies, D. H., Sawers, R. G., and Heberle, J. (2013) HypD is the scaffold protein for Fe-(CN)2CO cofactor assembly in [NiFe]-hydrogenase maturation. *Biochemistry* **52,** 3289–3296
29. Roseboom, W., Blokesch, M., Böck, A., and Albracht, S. P. (2005) The biosynthetic routes for carbon monoxide and cyanide in the Ni-Fe active site of hydrogenases are different. *FEBS Lett.* **579,** 469–472
30. Blokesch, M., Albracht, S. P., Matzanke, B. F., Drapal, N. M., Jacobi, A., and Böck, A. (2004) The complex between hydrogenase-maturation proteins HypC and HypD is an intermediate in the supply of cyanide to the active site iron of [NiFe]-hydrogenases. *J. Mol. Biol.* **344,** 155–167
31. Mizuno, Y., Ohba, Y., Fujita, H., Kanesaka, Y., Tamura, T., and Shiokawa, H. (1989) Activity staining of acylphosphatase after gel electrophoresis. *Anal. Biochem.* **183,** 46–49
32. Soboh, B., Kuhns, M., Braussemann, M., Waclawek, M., Muhr, E., Pierik, A. J., and Sawers, R. G. (2012) Evidence for an oxygen-sensitive iron-sulfur cluster in an immature large subunit species of *Escherichia coli* [NiFe]-hydrogenase 2. *Biochem. Biophys. Res. Commun.* **424,** 158–163
33. Theodoratou, E., Huber, R., and Böck, A. (2005) [NiFe]-hydrogenase maturation endopeptidase: structure and function. *Biochem. Soc. Trans.* **33,** 108–111
34. Volbeda, A., Charon, M. H., Piras, C., Hatchikian, E. C., Frey, M., and Fontecilla-Camps, J. C. (1995) Crystal structure of the nickel-iron hydrogenase from *Desulfovibrio gigas*. *Nature* **373,** 580–587
35. Drapal, N., and Bock, A. (1998) Interaction of the hydrogenase accessory protein HypC with HycE, the large subunit of *Escherichia coli* hydrogenase 3 during enzyme maturation. *Biochemistry* **37,** 2941–2948
36. Binder, U., Maier, T., and Böck, A. (1996) Nickel incorporation into hydrogenase 3 from *Escherichia coli* requires the precursor form of the large subunit. *Arch. Microbiol.* **165,** 69–72

37. Massanz, C., Fernandez, V. M., and Friedrich, B. (1997) C-terminal extension of the H2-activating subunit, HoxH, directs maturation of the NAD-reducing hydrogenase in *Alcaligenes eutrophus*. *Eur. J. Biochem.* **245,** 441–448
38. Watanabe, S., Matsumi, R., Atomi, H., Imanaka, T., and Miki, K. (2012) Crystal structures of the HypCD complex and the HypCDE ternary complex: transient intermediate complexes during [NiFe] hydrogenase maturation. *Structure* **20,** 2124–2137
39. Soboh, B., Krüger, S., Kuhns, M., Pinske, C., Lehmann, A., and Sawers, R. G. (2010) Development of a cell-free system reveals an oxygen-labile step in the maturation of [NiFe]-hydrogenase 2 of *Escherichia coli*. *FEBS Lett.* **584,** 4109–4114
40. Stripp, S. T., Lindenstrauss, U., Granich, C., Sawers, R. G., and Soboh, B. (2014) The influence of oxygen on [NiFe]-hydrogenase cofactor biosynthesis and how ligation of carbon monoxide precedes cyanation. *PLoS One* **9,** e107488
41. Friedrich, B., Buhrke, T., Burgdorf, T., and Lenz, O. (2005) A hydrogen-sensing multiprotein complex controls aerobic hydrogen metabolism in *Ralstonia eutropha*. *Biochem. Soc. Trans.* **33,** 97–101
42. Hedderich, R., and Forzi, L. (2005) Energy-converting [NiFe] hydrogenases: more than just H2 activation. *J. Mol. Microbiol. Biotechnol.* **10,** 92–104
43. Soboh, B., Linder, D., and Hedderich, R. (2002) Purification and catalytic properties of a CO-oxidizing:H2-evolving enzyme complex from *Carboxydothermus hydrogenoformans*. *Eur. J. Biochem.* **269,** 5712–5721
44. Soboh, B., Linder, D., and Hedderich, R. (2004) A multisubunit membrane-bound [NiFe] hydrogenase and an NADH-dependent Fe-only hydrogenase in the fermenting bacterium *Thermoanaerobacter tengcongensis*. *Microbiology* **150,** 2451–2463
45. Sorgenfrei, O., Linder, D., Karas, M., and Klein, A. (1993) A novel very small subunit of a selenium containing [NiFe] hydrogenase of *Methanococcus voltae* is postranslationally processed by cleavage at a defined position. *Eur. J. Biochem.* **213,** 1355–1358
46. Studier, F. W., and Moffatt, B. A. (1986) Use of bacteriophage T7 RNA polymerase to direct selective high-level expression of cloned genes. *J. Mol. Biol.* **189,** 113–130
47. Senger, M., Mebs, S., Duan, J., Wittkamp, F., Apfel, U. P., Heberle, J., Haumann, M., and Stripp, S. T. (2016) Stepwise isotope editing of [FeFe]-hydrogenases exposes cofactor dynamics. *Proc. Natl. Acad. Sci. U.S.A.* **113,** 8454–8459
48. Lukey, M. J., Parkin, A., Roessler, M. M., Murphy, B. J., Harmer, J., Palmer, T., Sargent, F., and Armstrong, F. A. (2010) How *Escherichia coli* is equipped to oxidize hydrogen under different redox conditions. *J. Biol. Chem.* **285,** 3928–3938
49. Laemmli, U. K. (1970) Cleavage of structural proteins during the assembly of the head of bacteriophage T4. *Nature* **227,** 680–685
50. Ballantine, S. P., and Boxer, D. H. (1985) Nickel-containing hydrogenase isoenzymes from anaerobically grown *Escherichia coli* K-12. *J. Bacteriol.* **163,** 454–459
51. Fish, W. W. (1988) Rapid colorimetric micromethod for the quantitation of complexed iron in biological samples. *Methods Enzymol.* **158,** 357–364
52. Menon, N. K., Chatelus, C. Y., Dervartanian, M., Wendt, J. C., Shanmugam, K. T., Peck, H. D., Jr., and Przybyla, A. E. (1994) Cloning, sequencing, and mutational analysis of the hyb operon encoding *Escherichia coli* hydrogenase 2. *J. Bacteriol* **176,** 4416–4423
53. Hube, M., Blokesch, M., and Böck, A. (2002) Network of hydrogenase maturation in Escherichia coli: role of accessory proteins HypA and HybF. *J. Bacteriol.* **184,** 3879–3885
54. Maier, T., Lottspeich, F., and Böck, A. (1995) Gtp hydrolysis by Hypb is essential for nickel insertion into hydrogenases of *Escherichia coli*. *Eur. J. Biochem.* **230,** 133–138
55. Khorasani-Motlagh, M., Lacasse, M. J., and Zamble, D. B. (2017) High-affinity metal binding by the *Escherichia coli* [NiFe]-hydrogenase accessory protein HypB is selectively modulated by SlyD. *Metallomics* **9,** 482–493
56. Shomura, Y., and Higuchi, Y. (2012) Structural basis for the reaction mechanism of *S*-carbamoylation of HypE by HypF in the maturation of [NiFe]-hydrogenases. *J. Biol. Chem.* **287,** 28409–28419
57. Petkun, S., Shi, R., Li, Y., Asinas, A., Munger, C., Zhang, L., Waclawek, M., Soboh, B., Sawers, R. G., and Cygler, M. (2011) Structure of hydrogenase maturation protein HypF with reaction intermediates shows two active sites. *Structure* **19,** 1773–1783
58. Casadaban, M. J. (1976) Transposition and fusion of *lac* genes to selected promoters in *Escherichia coli* using bacteriophage-λ and bacteriophage-μ. *J. Mol. Biol.* **104,** 541–555
59. Kitagawa, M., Ara, T., Arifuzzaman, M., Ioka-Nakamichi, T., Inamoto, E., Toyonaga, H., and Mori, H. (2005) Complete set of ORF clones of *Escherichia coli* ASKA library (a complete set of *E. coli* K-12 ORF archive): unique resources for biological research. *DNA Res.* **12,** 291–299
60. Barth, A. (2007) Infrared spectroscopy of proteins. *Biochim. Biophys. Acta* **1767,** 1073–1101
61. Bürstel, I., Siebert, E., Frielingsdorf, S., Zebger, I., Friedrich, B., and Lenz, O. (2016) CO synthesized from the central one-carbon pool as source for the iron carbonyl in O_2-tolerant [NiFe]-hydrogenase. *Proc. Natl. Acad. Sci. U.S.A.* **113,** 14722–14726